IEEE Access
Multidisciplinary ⋮ Rapid Review ⋮ Open Access Journal

Digital Object Identifier

Performance Analysis of Dual-Hop Wireless Systems Over Mixed FSO/RF Fading Channel

QIANG SUN[1], ZIHAN ZHANG[1], YAN ZHANG[2], MIGUEL LÓPEZ-BENÍTEZ[3], JIAYI ZHANG[1]
[1]School of Information Science and Technology, Nantong University, Nantong 226019, China. (e-mail: sunqiang@ntu.edu.cn).
[2]School of Electronic and Information Engineering, Beijing Jiaotong University, Beijing 100044, China.
[3]Department of Electrical Engineering and Electronics, University of Liverpool, Liverpool, L69 3GJ, United Kingdom, and also with the ARIES Research Centre, Antonio de Nebrija University, 28040 Madrid, Spain (e-mail: m.lopez-benitez@liverpool.ac.uk).

ABSTRACT This paper investigates the performance of a dual-hop mixed free-space optical (FSO)/radio frequency (RF) system. To this end, the FSO link is subject to the Gamma-Gamma distribution effects that account for pointing error impairments and under both heterodyne detection and intensity modulation with direct detection (IM/DD) methods, while the RF link undergoes the α-$\mathcal{F}$ distribution fading. For amplify-and-forward (AF) and decode-and-forward (DF) relaying, we derived the closed-form expressions of various important performance metrics by using bivariate Fox's H-functions, such as the average bit-error rate (BER), end-to-end outage probability (OP), effective capacity, and ergodic capacity. We unveil the effects of system and channel parameters on performance. Furthermore, we provide an asymptotical analysis to discuss significant diversity gains. Note that our results include previous works as special cases, which provides a framework. Finally, our derived expressions have confirmed the correctness via exactly matching Monte Carlo simulation results.

INDEX TERMS Free space optical communication, Gamma-Gamma, α-$\mathcal{F}$ fading, Dual-hop relaying.

I. INTRODUCTION

FREE space optical (FSO) communication systems are now growing many interests among researchers due to their superiority involving broader bandwidth and larger capacity confronted with the radio frequency (RF) systems. The FSO system applies light beams or laser technologies to improve the wireless network's effective connectivity, with operation in the unlicensed optical spectrum [1]–[3]. Besides, FSO systems serve as an alternative or supplement to the RF communication systems thanks to the ease of deployment and immunity to interference. These aforementioned superiorities of FSO transmission systems potentially allow settling the problem which the RF systems confront owing to the costly and spectrum shortage. It is a prospective technology because it provides full-duplex Gigabit Ethernet throughput in particular applications and environments contributing to a gigantic license-free spectrum, anti-jamming ability, and high security [4]. However, different atmospheric factors, such as rain, fog, aerosols, and mist, may cause atmospheric turbulence. Atmospheric turbulence can lead to undulation in both the intensity and the phase of the received signal due to a change in the refractive index along the way of communication [5]. This may cause a great deterioration in the capability of the FSO communication systems. Due to thermal dilation, dynamic wind loads, and weak earthquakes, the oscillation of the transmitter beam as well as misalignment between launcher and receiver owing to the construct swing phenomenon [6]. The pointing errors also can cause considerable performance worsening.

Additionally, the increasing demand for various high data rate applications has indicated in the past several years, fueled by the popularity of smartphones, tablets, and other intelligent devices. The cellular network and mobile hardware designers keeping on energetically extending the borders on the maximum data transfer rate where data can be communicated over wireless propagation channels [7]. Cisco's VNI predicts nearly exponential growth in the number of connected devices to roughly 12 billion and a sevenfold growth in cellular traffic to more than 40 exabytes per month by 2021 [8]. As one of the candidates for the future B5G network, the D2D wireless network uses the direct link between mobile user equipments (UEs) to reduce the burden on the base station (BS). Direct communication between mobile UEs can improve spectrum efficiency, but it also brings some

challenges, such as interference [9], [10].

A. RELATED WORKS

As an excellent solving method, relaying technology has been used at large in wireless communication systems mainly for the reason that it can offer wider and more power frugal coverage, as well as larger capacity in wireless networks [11]. Hybrid FSO/RF system, which was first proposed in [12], uses relay technology to integrate both the benefits of FSO and RF communication technology. The hybrid FSO/RF systems can further deploy to solve the connectivity gap which exists between the RF access network and the fiber optic-based backbone network [13], [14]. Therefore, quite a few researchers have invested considerable efforts in mixed FSO/RF systems employing both heterodyne and IM/DD detection with AF, DF, or CSI-Assisted Relaying. In [15]–[17], the performance of a hybrid FSO/RF system was studied over Gamma-Gamma and Nakagami-m fading channels. On the RF side, Generalized Nakagami-m, Fisher-Snedecor $\mathcal{F}$ fading, and fluctuating two-ray fading channels are assumed in [18]–[24], respectively. FSO link also was considered at the Double generalized gamma (DGG) fading channel because this model highly coincides with experimental results [13], [25]–[27]. The OP is derived for mixed RF/FSO systems using AF relay, where the channel is characterized by both Rayleigh fading and $\mathcal{M}$-distributed fading [28]. The authors in [29] derived an exact closed-form expression of the OP and the average BER of the same system model, in which the Rician and the generalized M*á*laga ($\mathcal{M}$) distributions are considered by the mmWave RF and FSO fading channels. In [30], the OP is derived for a mixed FSO/RF system using DF relay, where K distribution is utilized for modeling the FSO link and Rayleigh distribution utilized for modeling the RF link. The study of mixed FSO/RF system has been performed (from OP, ABER, and ergodic capacity points of view) in [31], where AF relay receives signals from the M*á*laga-$\mathcal{M}$/composite distributed FSO link and forwards these signals through the shadowing generalized-K (GK) distributed RF link. These studies above inspirit us to search for the diverse application scenarios of the FSO/RF system. We tackle the above problems by considering a hybrid FSO/RF system where RF link operates over the α-$\mathcal{F}$ distribution and applying to D2D communication. Very recently the authors in [32] put forward an up-to-date composite distribution which jointly considered both effects of undulation of dominant specular and the non-linearity of the communications medium, that is α-$\mathcal{F}$ distribution. This novel composite fading distribution yields a better fit to empirical data of D2D communications, compared with κ-μ shadowed, α-μ, and K distributions. Furthermore, α-$\mathcal{F}$ fading includes other well-known distributions (e.g., the Fisher-Snedocor $\mathcal{F}$, α-μ, and their inclusive ones), as special cases. Considering the α-$\mathcal{F}$ fading for the D2D link, it is mathematically more difficult to derive novel and accurate expressions for important performance metrics. Due to its highly consistent with the measured data, the α-$\mathcal{F}$ distribution also works well at underwater acoustic communications. In additions, the α-$\mathcal{F}$ distribution is prospective to be more beneficial than Nakagami-m and other available statistical models because of its flexibility. This is a highly potential issue that can be explored in the future. To the best of our knowledge, however, the performance of mixed RF/FSO transmission scheme over generalized Gamma-Gamma/α-$\mathcal{F}$ fading channels have not been investigated in the literature. In this paper, the main contributions are summarized as follows:

1) Using AF and DF relaying, the performance of the hybrid FSO/RF system is analyzed considering Gamma-Gamma distributed fading with the impact of both atmosphere turbulence and pointing error for the FSO links, while the RF link undergoes α-$\mathcal{F}$ fading channel. Note that our framework can generalize previous related works as special cases.
2) Novel closed-form expressions for several kinds of performance metrics, (e.g., the OP, average BER, ergodic capacity, and effective capacity) are given in terms of two-variate Fox's H-functions, which can be efficiently calculated with popular mathematical software.
3) Close asymptotic analyses of the derived OP and average BER in terms of common elementary functions in the high-SNR regime are also provided. More importantly, we present the diversity gain of the considered system to show the key impacts of system and channel parameters.

B. ORGANIZATION

The remaining part of the paper is organized as follows: Section II describes the system and channel models. The statistical characteristics of the end-to-end SNR of the links using AF and DF protocol are presented in Section III. In section IV, the derivations of accurate closed-form expressions and asymptotic results for several performance metrics are carried out. Section V provides simulation and numerical results. Finally, conclusions are given in Section VI.

II. SYSTEM AND CHANNEL MODELS

A. SYSTEM MODEL

We employ a dual-branch mixed FSO/RF system with relay-assisted. The relay node R, which uses both kinds of detection methods (IM/DD and heterodyne detection), is connected to source node S and destination terminal D as shown in Fig. 1. To handle the data rate mismatch between the FSO link and the RF link, the relay will be equipped with a buffer [33], [34] to temporarily store the data received from the first hop and forward it later through the second hop to the destination. The RF link in R and D is presumed to undergo an α-$\mathcal{F}$ fading distribution, which is more general and includes the α-μ ($m_s \rightarrow \infty$) and Fisher-Snedocor $\mathcal{F}$ ($\alpha = 2$) distributions as special cases [32]. The FSO link between S and R experiences a Gamma-Gamma fading

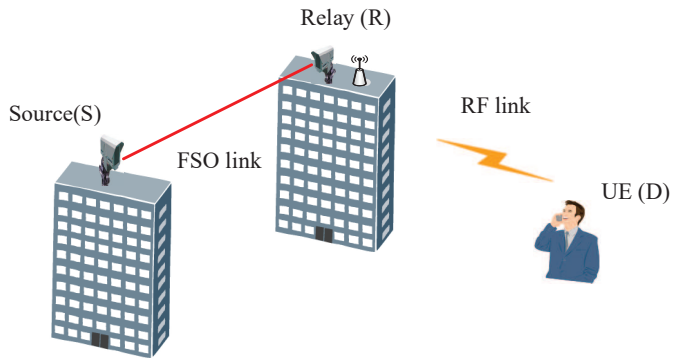

FIGURE 1. Mixed FSO/RF communication system model.

environment with pointing errors impairments[1].

B. END-TO-END SNR

Let the two links' instantaneous SNRs be represented by γ_{FSO} and γ_{RF}, respectively. Regardless of the fading amplitude on the first hop, the AF relay[2] will introduce a fixed gain into the received signal. On the grounds of the like analysis in [11], the end-to-end SNR can be expressed as

$$\gamma^{AF} = \frac{\gamma_{\text{FSO}}\gamma_{\text{RF}}}{\gamma_{\text{RF}} + C_R}, \tag{1}$$

where C_R is a parameter related to the fixed relay gain. In the DF relay scheme, the end-to-end SNR will be described as [27, Eq. (26)]

$$\gamma^{DF} = \min(\gamma_{FSO}, \gamma_{RF}), \tag{2}$$

C. FSO LINK

The probability density function (PDF) of γ_{FSO} is given by

$$f_{\gamma_{\text{FSO}}}(\gamma) = \frac{\xi^2}{r\gamma\Gamma(\alpha)\Gamma(\beta)} G_{1,3}^{3,0}\left(p\alpha\beta\left(\frac{\gamma}{\mu_r}\right)^{\frac{1}{r}} \middle| \begin{matrix} \xi^2+1 \\ \xi^2, \alpha, \beta \end{matrix}\right), \tag{3}$$

where $p = \frac{\xi^2}{\xi^2+1}$, $\gamma = (\eta_e \mathrm{I})^2/N_0$, η_e is the effective electrical-to-optical conversion ratio and I denote the receiver irradiance of FSO link which is given by $I = I_l I_a I_p$, where I_l, I_a, and I_p represent the path loss, the effect of atmospheric turbulence, and the pointing error caused by building sway, respectively. Without loss of generality, I_l is deterministic ($I_l = 1$ will be used in this paper) [35]. The parameter r decides the method of detection being employed (i.e., $r=1$ denotes heterodyne detection and $r=2$ connected with IM/DD), μ_r stands for the average electrical SNR of the FSO link. To be specific, for $r=1$, $\mu_1 = \overline{\gamma_1} = \mu_{heterodyne}$, and for $r=2$, $\mu_2 = \overline{\gamma_1}\frac{\alpha\beta\xi^2(\xi^2+2)}{(\alpha+1)(\beta+1)(\xi^2+1)^2} = \mu_{IM/DD}$. At the receiver, the ratio between the equivalent beam radius and the pointing error displacement standard deviation (jitter) expressed as $\xi = \frac{\omega_{z_{eq}}}{2\sigma_s}$ ($\xi \to \infty$ means negligible pointing errors), with ${\sigma_s}^2$ and $\omega_{z_{eq}}$ are the jitter variance and the equivalent beam radius, respectively [20]. Moreover, in (3), $\Gamma(\cdot)$ [36, Eq. (8.310)] and $G_{p,q}^{m,n}[\cdot]$ [36, Eq. (9.301)] represent the Gamma and the Meijer's G-function functions, respectively. The characteristic parameters α and β are defined as the valid numbers of small-scale and large-scale cells, respectively, associated with atmospheric turbulence. Alternatively, for the case of plane wave propagation, α and β can be straight related to physical parameters, when the lack of inner scale [18].

$$\alpha = \left[\exp\left(\frac{0.49\sigma_c^2}{\left(1+1.11\sigma_c^{12/5}\right)^{7/6}}\right) - 1\right]^{-1} \tag{4}$$

$$\beta = \left[\exp\left(\frac{0.51\sigma_c^2}{\left(1+0.69\sigma_c^{12/5}\right)^{5/6}}\right) - 1\right]^{-1} \tag{5}$$

where $\sigma_C^2 = 1.23\widehat{k}^{\frac{7}{6}} C_n^2 L^{\frac{11}{6}}$ is the Rytov variance, C_n^2 denotes the refractive-index structure parament, L is the propagation distance, and $\widehat{k} \triangleq \frac{2\pi}{\lambda}$ is the wave number where λ represents the wavelength. Utilizing $F_{\gamma_{\text{FSO}}}(\gamma) \triangleq \int_0^{\gamma} f_{\gamma_{\text{FSO}}}(x)dx$, [37, Eq. (2.91)], [38, Eq. (1.59), Eq. (2.54)], and after some mathematical manipulations, then the cumulative distribution function (CDF) of the instantaneous SNR γ_{FSO} under Gamma-Gamma fading can be determined as

$$\begin{aligned} F_{\gamma_{\text{FSO}}}(\gamma) &= 1 - \frac{\xi^2}{\Gamma(\alpha)\Gamma(\beta)} \\ &\times H_{2,4}^{4,0}\left(\frac{(\alpha\beta)^r}{\mu_r}\gamma \middle| \begin{matrix} \left(\xi^2+1, r\right), (1,1) \\ (0,1), \left(\xi^2, r\right), (\alpha, r), (\beta, r) \end{matrix}\right), \end{aligned} \tag{6}$$

where $H(\cdot)$ is the Fox's H-function [37, Eq. (1.1.1)].

D. RF LINK

Assuming that γ_{RF} follows the α-$\mathcal{F}$ distribution, the PDF is given by [32, Eq. (3)]

$$\begin{aligned} f_{\gamma_{\text{RF}}}(\gamma) &= \frac{a}{2B(\mu, m_s)}\left(\frac{(m_s-1)\overline{\gamma}^{\frac{a}{2}}}{\mu\lambda^{\frac{a}{2}}}\right)^{m_s} \gamma^{\frac{a\mu}{2}-1} \\ &\times \left(\gamma^{\frac{a}{2}} + \frac{(m_s-1)\overline{\gamma}^{\frac{a}{2}}}{\mu\lambda^{\frac{a}{2}}}\right)^{-(\mu+m_s)}, \end{aligned} \tag{7}$$

where $B(\cdot,\cdot)$ is the beta function as defined in [36, Eq. (8.380)] and

$$\lambda = \left(\frac{m_s-1}{\mu}\right)^{\frac{2}{a}} \frac{\Gamma(\mu+\frac{2}{a})\Gamma(m_s-\frac{2}{a})}{\Gamma(\mu)\Gamma(m_s)}, m_s > \frac{2}{a}. \tag{8}$$

By substituting (7) into $F_{\gamma_{\text{RF}}}(\gamma) \triangleq \int_0^{\gamma} f_{\gamma_{\text{RF}}}(x)dx$ and using the change of variable $t = \gamma^{\frac{a}{2}}$ [36, Eq. (3.194.3)], CDF of γ_{RF} can be written as

$$\begin{aligned} F_{\gamma_{\text{RF}}}(\gamma) &= 1 - \frac{1}{m_s B(\mu, m_s)}\left(\frac{(m_s-1)\overline{\gamma}^{\frac{a}{2}}}{\mu\lambda^{\frac{a}{2}}}\right)^{m_s} \gamma^{-\frac{am_s}{2}} \\ &{}_2F_1\left(\mu+m_s, m_s; m_s+1; -\frac{(m_s-1)\overline{\gamma}^{\frac{a}{2}}}{\mu\lambda^{\frac{a}{2}}\gamma^{\frac{a}{2}}}\right), \end{aligned} \tag{9}$$

[1]The effect of non-zero boresight pointing errors is will be addressed in our future work.

[2]In this paper, we assume that perfect decoding at both relay and destination. The effect of erroneous decoding at relay and destination will be considered as part of the future works.

Using [39, Eq. (16.18.1), [Eq. (16.19.2)] and with some algebraic manipulations, the CDF of the α-$\mathcal{F}$ distribution (9) becomes

$$F_{RF}(\gamma) = 1 - \frac{G_{2,2}^{1,2}\left(\frac{(m_s-1)\bar{\gamma}^{\frac{a}{2}}}{\mu\lambda^{\frac{a}{2}}\gamma^{\frac{a}{2}}} \middle| \begin{matrix} 1-\mu, 1 \\ m_s, 0 \end{matrix}\right)}{\Gamma(\mu)\Gamma(m_s)}, \quad (10)$$

where μ denotes the number of multipath clusters, a represents the non-linearity of the propagation medium, m_s is the shadowing parameter.

III. STATISTICS OF END-TO-END SNR

In this section, we will present the exact and useful statistics of the end-to-end SNRs, which are useful for deriving the significant performance metrics of the considered system.

A. AF RELAY WITH FIXED-GAIN

Proposition 1. *The end-to-end SNR CDF for a dual-hop mixed FSO/RF system using AF relay with fixed-gain can be derived in closed-form in terms of the Fox's H-function of two variables as shown*

$$F_{\gamma^{AF}}(\gamma) = 1 - \frac{\xi^2}{r\Gamma(\alpha)\Gamma(\beta)}\frac{1}{\Gamma(m)\Gamma(\mu)} H_{1,0:2,3:3,2}^{0,1:3,1:0,3} \times \left[\begin{matrix} \left(1, \frac{a}{2}, \frac{1}{r}\right) \\ - \\ (1-m_s, 1)(1,1) \\ (\mu, 1)\,(0,1)\,\left(1, \frac{a}{2}\right) \\ \left(1-\xi^2, 1\right)(1-\alpha, 1)(1-\beta, 1) \\ \left(-\xi^2, 1\right)\left(0, \frac{1}{r}\right) \end{matrix} \middle| \begin{matrix} \\ \\ \\ \frac{\mu\lambda^{\frac{a}{2}} C_R{}^{\frac{a}{2}}}{(m_s-1)\bar{\gamma}^{\frac{a}{2}}}, \frac{\left(\frac{\mu_r}{\gamma}\right)^{\frac{1}{r}}}{\alpha\beta} \\ \\ \\ \end{matrix} \right]. \quad (11)$$

Proof: Please see Appendix A. ■

Here, $H_{p1,q1:p2,q2:p3,q3}^{0,n1:m2,n2:m3,n3}[\cdot]$ is bivariate Fox's-H function in (11), through well-known software like MATHEMATICA, which can be calculated numerically [40]. The MATLAB implementation of this function is outlined in [41]. It is worth to point out that for $\alpha = 2$, $m_s \to \infty$, $r = 2$ and $\xi \to \infty$, (11) can be reduced to the CDF of the hybrid relaying systems where IM/DD is operated under the FSO link without pointing errors and the RF link is characterized by Nakagami-m fading. Additionally, by setting $\alpha = 2$, $m_s \to \infty$, $r = 1$, and using [37, Eq. (2.9.1)], the CDF reduces to [15, Eq. (7)] which was earlier obtained for mixed Gamma-Gamma/Nakagami-m systems with pointing errors under heterodyne detection.

The exact expression of the CDF is a fairly complex function that shows limited physical insights. Therefore, it has practical significance to derive an asymptotic analysis of the CDF in the high average SNR regime. By utilizing [40, Eq. (1.1)], [37, Th.1.7 and Th.1.11] along with [37, Eq. (1.59) , Eq. (1.84)] and after some algebraic manipulations, (11) yields the following asymptotic expression

$$F_{\gamma^{AF}}(\gamma) \approx \frac{\xi^2}{\Gamma(\alpha)\Gamma(\beta)\Gamma(m)\Gamma(\mu)} \sum_{i=1}^{4} \Xi_i {\mu_r}^{-\theta_i}, \quad (12)$$

where $\theta_i = \{\frac{a\mu}{2}, \frac{\xi^2}{2}, \frac{\alpha}{2}, \frac{\beta}{2}\}$

$$\Xi_1 = \frac{\Gamma(m_s+\mu)\Gamma(\alpha-\frac{a\mu r}{2})\Gamma(\beta-\frac{a\mu r}{2})}{\mu^{\mu-1}(\xi^2-\frac{a\mu r}{2})} \left(\frac{\left(\frac{(\alpha\beta)^r\lambda C_R\gamma}{\bar{\gamma}}\right)^{\frac{a}{2}}}{(m_s-1)}\right)^{\mu}, \quad (13)$$

$$\Xi_2 = \frac{\Gamma(\alpha-\xi^2)\Gamma(\beta-\xi^2)}{\xi^2}\left(\alpha\beta(\gamma)^{\frac{1}{r}}\right)^{\xi^2} \times(\xi^2\Gamma(m_s+\tfrac{2}{a})\Gamma(\mu-\tfrac{2}{a})\left(\frac{\lambda C_R}{\bar{\gamma}}\left(\frac{\mu}{m_s-1}\right)^{\frac{2}{a}}\right) + \frac{\xi^2\Gamma(m_s+\mu)\Gamma(1-\frac{a\mu}{2})\Gamma(\frac{a\mu}{2}-\frac{\xi^2}{r})}{\mu\Gamma(1-\frac{\xi^2}{r})}\left(\frac{\lambda C_R}{\bar{\gamma}}\left(\frac{\mu}{m_s-1}\right)^{\frac{2}{a}}\right)^{\mu} + \frac{\Gamma(m_s+\frac{2\xi^2}{ar})\Gamma(\mu-\frac{2\xi^2}{ar})}{2}\left(\frac{\lambda C_R}{\bar{\gamma}}\left(\frac{\mu}{m_s-1}\right)^{\frac{2}{a}}\right)^{\frac{\xi^2}{r}} + \Gamma(m_s)\Gamma(\mu)), \quad (14)$$

$$\Xi_3 = \frac{\Gamma(\beta-\alpha)}{\alpha(\xi^2-\alpha)}\left(\alpha\beta(\gamma)^{\frac{1}{r}}\right)^{\alpha} \times(\alpha\Gamma(m_s+\tfrac{2}{a})\Gamma(\mu-\tfrac{2}{a})\left(\frac{\lambda C_R}{\bar{\gamma}}\left(\frac{\mu}{m_s-1}\right)^{\frac{2}{a}}\right) + \frac{\alpha\Gamma(m_s+\mu)\Gamma(1-\frac{a\mu}{2})\Gamma(\frac{a\mu}{2}-\frac{\alpha}{r})}{\mu\Gamma(1-\frac{\alpha}{r})}\left(\frac{\lambda C_R}{\bar{\gamma}}\left(\frac{\mu}{m_s-1}\right)^{\frac{2}{a}}\right)^{\mu} + \frac{\Gamma(m_s+\frac{2\alpha}{ar})\Gamma(\mu-\frac{2\alpha}{ar})}{2}\left(\frac{\lambda C_R}{\bar{\gamma}}\left(\frac{\mu}{m_s-1}\right)^{\frac{2}{a}}\right)^{\frac{\alpha}{r}} + \Gamma(m_s)\Gamma(\mu)), \quad (15)$$

$$\Xi_4 = \frac{\Gamma(\alpha-\beta)}{\beta(\xi^2-\beta)}\left(\alpha\beta(\gamma)^{\frac{1}{r}}\right)^{\beta} \times(\beta\Gamma(m_s+\tfrac{2}{a})\Gamma(\mu-\tfrac{2}{a})\left(\frac{\lambda C_R}{\bar{\gamma}}\left(\frac{\mu}{m_s-1}\right)^{\frac{2}{a}}\right) + \frac{\beta\Gamma(m_s+\mu)\Gamma(1-\frac{a\mu}{2})\Gamma(\frac{a\mu}{2}-\frac{\beta}{r})}{\mu\Gamma(1-\frac{\beta}{r})}\left(\frac{\lambda C_R}{\bar{\gamma}}\left(\frac{\mu}{m_s-1}\right)^{\frac{2}{a}}\right)^{\mu} + \frac{\Gamma(m_s+\frac{2\beta}{ar})\Gamma(\mu-\frac{2\beta}{ar})}{2}\left(\frac{\lambda C_R}{\bar{\gamma}}\left(\frac{\mu}{m_s-1}\right)^{\frac{2}{a}}\right)^{\frac{\beta}{r}} + \Gamma(m_s)\Gamma(\mu)). \quad (16)$$

Proof: Please see Appendix B. ■

B. DF RELAYING

Proposition 2. *Based on* (2)*, the CDF of the equivalent end-to-end SNR γ_{DF} at the destination can be formulated in terms of individual CDFs as [42, Eq. (4)]*

$$F_{\gamma^{DF}}(\gamma) = F_{\gamma_{FSO}}(\gamma) + F_{\gamma_{RF}}(\gamma) - F_{\gamma_{FSO}}(\gamma)\,F_{\gamma_{RF}}(\gamma) = 1 - F^C_{\gamma_{FSO}}(\gamma)\,F^C_{\gamma_{RF}}(\gamma), \quad (17)$$

where $F^C_{\gamma}(\cdot)$ is defined as complementary CDF (CCDF) of γ. It is clear that the CDF of mixed FSO/RF systems employing DF relay can be expressed as

$$F_{\gamma^{DF}}(\gamma) = 1 - \frac{1}{\Gamma(\mu)\Gamma(m_s)}\frac{\xi^2}{\Gamma(\alpha)\Gamma(\beta)} \times H_{2,2}^{1,2}\left(\frac{(m_s-1)\bar{\gamma}^{\frac{a}{2}}}{\mu\lambda^{\frac{a}{2}}\gamma^{\frac{a}{2}}} \middle| \begin{matrix} (1-\mu,1),(1,1) \\ (m_s,1)(0,1) \end{matrix}\right) \times H_{2,4}^{4,0}\left(\frac{(\alpha\beta)^r}{\mu_r}\gamma \middle| \begin{matrix} \left(\xi^2+1, r\right),(1,1) \\ (0,1),\left(\xi^2, r\right),(\alpha, r),(\beta, r) \end{matrix}\right). \quad (18)$$

Proof: By substituting (6) and (10) into (17), then the CDF is obtained as in (18) after some manipulations. Thus, the proof is completed. ■

In the high average SNRs, by applying [37, Eq. (1.59)] to (18), the CDF of the end-to-end SNR for DF relaying in the high-SNR regime can be given by

$$F_{\gamma_{DF}}^{\infty}(\gamma) = F_{\gamma_{\text{FSO}}}^{\infty}(\gamma) + F_{\gamma_{\text{RF}}}^{\infty}(\gamma) - F_{\gamma_{\text{FSO}}}^{\infty}(\gamma) F_{\gamma_{\text{RF}}}^{\infty}(\gamma), \quad (19)$$

where

$$\begin{aligned} F_{\gamma_{\text{FSO}}}^{\infty}(\gamma) &= \frac{r\Gamma\left(\alpha-\xi^2\right)\Gamma\left(\beta-\xi^2\right)}{\Gamma(\alpha)\Gamma(\beta)}\left(\frac{(\alpha\beta)^r}{\mu_r}\gamma\right)^{\frac{\xi^2}{r}} \\ &+\frac{r\xi^2\Gamma\left(\xi^2-\alpha\right)\Gamma(\beta-\alpha)}{\alpha\Gamma(\alpha)\Gamma(\beta)\Gamma(\xi^2+1-\alpha)}\left(\frac{(\alpha\beta)^r}{\mu_r}\gamma\right)^{\frac{\alpha}{r}} \\ &+\frac{r\xi^2\Gamma\left(\xi^2-\beta\right)\Gamma(\alpha-\beta)}{\beta\Gamma(\alpha)\Gamma(\beta)\Gamma(\xi^2+1-\beta)}\left(\frac{(\alpha\beta)^r}{\mu_r}\gamma\right)^{\frac{\beta}{r}}, \end{aligned} \quad (20)$$

$$F_{\gamma_{\text{RF}}}^{\infty}(\gamma) = \frac{\mu^{\mu-1}}{B(\mu,m_s)}\left(\frac{1}{(m_s-1)}\left(\frac{\lambda\gamma}{\overline{\gamma}}\right)^{\frac{a}{2}}\right)^{\mu}. \quad (21)$$

IV. PERFORMANCE ANALYSIS

A. OUTAGE PROBABILITY

The quality of service (QoS) is guaranteed by remaining the instantaneous SNR γ. The probability that the γ declines under a predetermined protection ratio γ_{th} is defined as the outage probability. We can get the outage probability by substituting γ_{th} into (11) and (18) as

$$P_{out}(\gamma_{\text{th}}) = P_r[\gamma < \gamma_{\text{th}}] = F_{\gamma}(\gamma_{\text{th}}). \quad (22)$$

B. AVERAGE BIT-ERROR RATE

In addition to the possibility of interruption, average BER is another important indicator of system performance. Using the approach recommended in [43], the BER for most binary modulations can be written as

$$\bar{P}_e = \frac{\delta}{2\Gamma(p)}\sum_{k=1}^{n} q_k^p \int_0^{\infty} \gamma^{p-1}\exp(-q_k\gamma)F_{\gamma}(\gamma)\,d\gamma \quad (23)$$

where δ, n, p, q_k are parameters with values that depend on the type of the digital modulation scheme. As summarized in [43, Table 1], the average BER for coherent binary frequency shift keying (CBFSK) is given by (23) with $(\delta, n, p, q_k) = (1, 1, 0.5, 0.5)$ and $(\delta, n, p, q_k) = (1, 1, 1, 1)$ denotes coherent binary phase shift keying (DBPSK).

1) Fixed-Gain AF Relaying

By substituting (11) into (23), the ABER is given as

$$\overline{P}_e^{AF} = \frac{n\delta}{2} - \frac{\delta}{2\Gamma(p)}\frac{\xi^2}{r\Gamma(\alpha)\Gamma(\beta)}\frac{1}{\Gamma(\mu)\Gamma(m_s)}\sum_{k=1}^{n} H_{1,0:2,3:3,3}^{0,1:3,1:1,3} \times \left[\begin{matrix} \left(1,\frac{a}{2},\frac{1}{r}\right) \\ - \\ (1-m_s,1)(1,1) \\ (\mu,1)\,(0,1)\,\left(1,\frac{a}{2}\right) \\ \left(1-\xi^2,1\right)(1-\alpha,1)(1-\beta,1) \\ \left(p,\frac{1}{r}\right)\left(-\xi^2,1\right)\left(0,\frac{1}{r}\right) \end{matrix}\middle| \begin{matrix} \\ \\ \\ \frac{\mu\lambda^{\frac{a}{2}}C_R^{\frac{a}{2}}}{(m_s-1)\overline{\gamma}^{\frac{a}{2}}}, \frac{(q_k\mu_r)^{\frac{1}{r}}}{\alpha\beta} \\ \\ \\ \end{matrix}\right]. \quad (24)$$

Proof: Please see Appendix C. ■

It is important to point out that for $\alpha = 2$, $m_s \to \infty$, $r = 2$, $n = 1$, $\delta = 1$ and $\xi \to \infty$, (24) simplifies to the average BER of the mixed dual-hop relaying systems where IM/DD is operated under the FSO link and the RF link suffers Nakagami-m fading model. In addition, by setting $\alpha = 2$, $m_s \to \infty$, $r = 1$, $n = 1$ and $\delta = 1$, the average BER in (24) reduces to [18, Eq. (13)] which was earlier obtained for mixed Gamma-Gamma/Nakagami-m systems using heterodyne detection with pointing errors. The slope of the BEP and OP versus the average SNR curve at a high SNR regime on a logarithmic scale is defined as the diversity order. Without loss of generality, we presume $\overline{\gamma_1} \triangleq v\mu_r \triangleq \overline{\gamma}$ $(\mu_r, \bar{\gamma} \to \infty)$, in which v represents a positive constant [44]. By using [40, Eq. (1.1)], [37, Th.1.7 and Th.1.11] along with [37, Eq. (1.59), Eq. (1.84)] and after some algebraic manipulations, (24) yields the following asymptotic expression

$$\overline{P}_e^{AF} \approx \frac{\delta\xi^2}{2\Gamma(\alpha)\Gamma(\beta)\Gamma(m)\Gamma(\mu)}\sum_{i=1}^{4}\phi_i\Gamma(p+\theta_i), \quad (25)$$

where

$$\phi_1 = \frac{\Gamma(ms+\mu)\Gamma(\alpha-\frac{a\mu r}{2})\Gamma(\beta-\frac{a\mu r}{2})}{\mu^{\mu-1}(\xi^2-\frac{a\mu r}{2})}\left(\frac{(\alpha\beta)^{\frac{ar}{2}}(\lambda C_R\gamma)^{\frac{a}{2}}}{(m_s-1)(q_k)^{\frac{1}{r}}(\overline{\gamma_1})^{\frac{1}{r}+\frac{a}{2}}}\right)^{\mu}, \quad (26)$$

$$\begin{aligned} \phi_2 &= \frac{\Gamma(\alpha-\xi^2)\Gamma(\beta-\xi^2)}{(q_k\overline{\gamma_1})^{\frac{\xi^2}{r}}} \\ &\times\Big(\frac{\Gamma(m_s+\frac{2\xi^2}{ar})\Gamma(\mu-\frac{2\xi^2}{ar})}{2\xi^2}\left(\left(\frac{(\alpha\beta)^r\lambda C_R}{\overline{\gamma_1}}\right)^{\frac{a}{2}}\frac{\mu}{(m_s-1)}\right)^{\xi^2} \\ &+(\alpha\beta)^{\xi^2}\times\frac{\Gamma(m_s+\mu)\Gamma(1-\frac{a\mu}{2})\Gamma(\frac{a\mu}{2}-\frac{\xi^2}{r})}{\mu\Gamma(1-\frac{\xi^2}{r})}\left(\left(\frac{\lambda C_R}{\overline{\gamma_1}}\right)^{\frac{a}{2}}\frac{\mu}{m_s-1}\right)^{\mu} \\ &+\Big(\Gamma(m_s+\frac{2}{a})\Gamma(\mu-\frac{2}{a})\left(\frac{\lambda C_R}{\overline{\gamma_1}}\left(\frac{\mu}{m_s-1}\right)^{\frac{2}{a}}\right)+\frac{\Gamma(m_s)\Gamma(\mu)}{\xi^2}\Big)\Big), \end{aligned} \quad (27)$$

$$\begin{aligned} \phi_3 &= \frac{\Gamma(\beta-\alpha)}{(\xi^2-\alpha)(q_k\overline{\gamma_1})^{\frac{\alpha}{r}}} \\ &\times\Big(\frac{\Gamma(m_s+\frac{2\alpha}{ar})\Gamma(\mu-\frac{2\alpha}{ar})}{2\alpha}\left(\left(\frac{(\alpha\beta)^r\lambda C_R}{\overline{\gamma_1}}\right)^{\frac{a}{2}}\frac{\mu}{(m_s-1)}\right)^{\alpha} \\ &+(\alpha\beta)^{\alpha}\times\Big(\frac{\Gamma(m_s+\mu)\Gamma(1-\frac{a\mu}{2})\Gamma(\frac{a\mu}{2}-\frac{\alpha}{r})}{\mu\Gamma(1-\frac{\alpha}{r})}\left(\left(\frac{\lambda C_R}{\overline{\gamma_1}}\right)^{\frac{a}{2}}\frac{\mu}{m_s-1}\right)^{\mu} \\ &+\Big(\Gamma(m_s+\frac{2}{a})\Gamma(\mu-\frac{2}{a})\left(\frac{\lambda C_R}{\overline{\gamma_1}}\left(\frac{\mu}{m_s-1}\right)^{\frac{2}{a}}\right)+\frac{\Gamma(m_s)\Gamma(\mu)}{\alpha}\Big), \end{aligned} \quad (28)$$

$$\begin{aligned} \phi_4 &= \frac{\Gamma(\alpha-\beta)}{(\xi^2-\beta)(q_k\overline{\gamma_1})^{\frac{\beta}{r}}} \\ &\times\frac{\Gamma(m_s+\frac{2\beta}{ar})\Gamma(\mu-\frac{2\beta}{ar})}{2\beta}\left(\left(\frac{(\alpha\beta)^r\lambda C_R}{\overline{\gamma_1}}\right)^{\frac{a}{2}}\frac{\mu}{(m_s-1)}\right)^{\beta} \\ &+(\alpha\beta)^{\beta}\times\frac{\Gamma(m_s+\mu)\Gamma(1-\frac{a\mu}{2})\Gamma(\frac{a\mu}{2}-\frac{\beta}{r})}{\mu\Gamma(1-\frac{\beta}{r})}\left(\left(\frac{\lambda C_R}{\overline{\gamma_1}}\right)^{\frac{a}{2}}\frac{\mu}{m_s-1}\right)^{\mu} \\ &+\Big(\Gamma(m_s+\frac{2}{a})\Gamma(\mu-\frac{2}{a})\left(\frac{\lambda C_R}{\overline{\gamma_1}}\left(\frac{\mu}{m_s-1}\right)^{\frac{2}{a}}\right)+\frac{\Gamma(m_s)\Gamma(\mu)}{\beta}\Big). \end{aligned} \quad (29)$$

Using [45, Eq. (1)], the diversity order can be equal to

$$G_d = \min\left(\frac{a\mu}{2}+\frac{\mu}{r},\frac{\xi^2}{r},\frac{\alpha}{r},\frac{\beta}{r}\right). \quad (30)$$

2) DF Relaying

The closed-form expression of the average BER, by substituting (18) into (23), [46, (2.25.1/1)] and the similar method aforementioned, can be derived as

$$\overline{P}_e^{DF} = \frac{n\delta}{2} - \frac{\delta}{2\Gamma(p)} \frac{\xi^2}{\Gamma(\alpha)\Gamma(\beta)} \frac{1}{\Gamma(\mu)\Gamma(m_s)} \sum_{k=1}^{n} H_{1,0:2,2:2,4}^{0,1:2,1:4,0} \times \left[\begin{matrix} \left(1-p, \frac{a}{2}, 1\right) \\ - \\ (1-m_s, 1)(1,1) \\ (\mu, 1)\,(0,1) \\ \left(1+\xi^2, r\right)(1,1) \\ \left(\xi^2, r\right)(\alpha, r)\,(\beta, r)\,(0,1) \end{matrix} \middle| \begin{matrix} \\ \\ \frac{\mu \lambda^{\frac{a}{2}}}{(m_s-1)\overline{\gamma}^{\frac{a}{2}} q_k^{\frac{a}{2}}}, \frac{(\alpha\beta)^r}{q_k \mu_r} \end{matrix} \right]. \tag{31}$$

The asymptotic form expression for the average BER in (31) can be derived through talking $\mu_r \gg 1$, $\overline{\gamma} \gg 1$, in (18), and substituting (17) into (23) with some algebraic manipulation.

$$\begin{aligned} \overline{P}_e^{DF} &= \frac{\delta}{2\Gamma(p)} \sum_{k=1}^{n} \frac{r\Gamma\left(\alpha-\xi^2\right)\Gamma\left(\beta-\xi^2\right)\Gamma\left(p+\frac{\xi^2}{r}\right)}{\Gamma(\alpha)\Gamma(\beta)} \left(\frac{(\alpha\beta)^r}{\mu_r q_k}\right)^{\frac{\xi^2}{r}} \\ &+ \frac{\delta}{2\Gamma(p)} \sum_{k=1}^{n} \frac{r\xi^2\Gamma\left(\xi^2-\alpha\right)\Gamma(\beta-\alpha)\Gamma\left(p+\frac{\alpha}{r}\right)}{\alpha\Gamma(\alpha)\Gamma(\beta)\Gamma(\xi^2+1-\alpha)} \left(\frac{(\alpha\beta)^r}{\mu_r q_k}\right)^{\frac{\alpha}{r}} \\ &+ \frac{\delta}{2\Gamma(p)} \sum_{k=1}^{n} \frac{r\xi^2\Gamma\left(\xi^2-\beta\right)\Gamma(\alpha-\beta)\Gamma\left(p+\frac{\beta}{r}\right)}{\beta\Gamma(\alpha)\Gamma(\beta)\Gamma(\xi^2+1-\beta)} \left(\frac{(\alpha\beta)^r}{\mu_r q_k}\right)^{\frac{\beta}{r}} \\ &+ \frac{\delta}{2\Gamma(p)} \sum_{k=1}^{n} \frac{\mu^{\mu-1}\Gamma\left(\frac{a\mu}{2}+p\right)}{B(\mu, ms)} \left(\frac{\lambda^{\frac{a}{2}}}{(m_s-1)\overline{\gamma}^{\frac{a}{2}} q_k^{\frac{a}{2}}}\right)^{\mu}. \end{aligned} \tag{32}$$

Furthermore, the diversity gain is found as

$$G_d = \min\left(\frac{a\mu}{2}, \frac{\xi^2}{r}, \frac{\alpha}{r}, \frac{\beta}{r}\right). \tag{33}$$

C. ERGODIC CAPACITY

1) Fixed-Gain AF Relaying

From [47] the ergodic capacity of the considered FSO/RF system operating under heterodyne and IM/DD techniques can be written as

$$\overline{C} \triangleq \frac{1}{2}\mathbb{E}\left[\log_2\left(1+c\gamma\right)\right] = \frac{c}{2\ln(2)} \int_0^{\infty} \frac{F_{\gamma}^{c}(\gamma)}{1+c\gamma} d\gamma. \tag{34}$$

where $\mathbb{E}(\cdot)$ represents the expectation operator. c is a constant, where $c=1$ is associated with the heterodyne detection (i.e., $r=1$) and $c = e/2\pi$ stands for the IM/DD technique (i.e., $r=2$).

Proposition 3. *The ergodic capacity of the mixed FSO/RF systems can be derived as* (35)*, seeing the top of the next page.*

Proof: Substituting (11) into (34), using [36, Eq. (4.293/10)] the ergodic capacity can be written as

$$\begin{aligned} \overline{C}^{AF} &= \frac{\xi^2}{2r\ln(2)\Gamma(\alpha)\Gamma(\beta)\Gamma(\mu)\Gamma(m_s)} \left(\frac{1}{2\pi i}\right)^2 \\ &\times \int_{L_1} \frac{\Gamma(\xi^2+t)\Gamma(\alpha+t)\Gamma(\beta+t)\Gamma(1-\frac{t}{r})\Gamma(\frac{t}{r})}{\Gamma(\xi^2+1+t)\Gamma(1+\frac{t}{r})} \left(\frac{(\mu_r)^{\frac{1}{r}}}{\alpha\beta}\right)^{t} dt \\ &\times \int_{L_2} \frac{\Gamma(m_s+s)\Gamma(\mu-s)\Gamma(-s)\Gamma(1-\frac{as}{2})}{\Gamma(1-s)} \Gamma\left(\frac{t}{r}+\frac{as}{2}\right) \left(\frac{\mu(\lambda C_R)^{\frac{a}{2}}}{(ms-1)\overline{\gamma}^{\frac{a}{2}}}\right)^{s} ds. \end{aligned} \tag{36}$$

The proof is completed with the help of [40, Eq. (1.1)]. ■

For $a=2$, $m_s=\infty$, $r=1$, the ergodic capacity in (35) reduces to [18, Eq. (15)]. Moreover, when we set $a=2$, $m_s=\infty$, $r=2$ and $\xi=\infty$, (35) reduces to the ergodic capacity of the mixed FSO/RF systems as the special case where IM/DD is operated under the FSO link with no pointing errors and the RF link undergoes Nakagami-m fading model.

2) DF Relaying

By using [38, Eq. (1.43)], [46, Eq. (2.25.1/1)], [40, Eq.(2.3)] and substituting (17) into (34), the ergodic capacity of DF relaying can be written as (37), seeing the top of the next page.

D. EFFECTIVE CAPACITY

1) Fixed-Gain AF Relaying

The effective capacity can be expressed as

$$\begin{aligned} R &\triangleq -\tfrac{1}{A}\log_2(\mathbb{E}\{1+\gamma\}^{-A}) \\ &= -\tfrac{1}{A}\log_2\left(1 - A\int_0^{\infty}(1+\gamma)^{-A-1} F_{\gamma}^{C}(\gamma) d\gamma\right), \end{aligned} \tag{38}$$

where $A \triangleq \theta TB/ln2$ with the block length T, the asymptotic reduce speed of the buffer occupancy θ, and the system bandwidth B [20].

Proposition 4. *The effective capacity of the dual-hop FSO/RF systems can be formulated as (38), seeing the bottom of the next page.*

Proof: Substituting (11) into (38), using [36, Eq. (3.194/3)] the effective capacity can be written as

$$\begin{aligned} R^{AF} &= -\tfrac{1}{A}\log_2\Big(1 - \frac{A\xi^2}{r\Gamma(\alpha)\Gamma(\beta)\Gamma(\mu)\Gamma(m_s)} \left(\frac{1}{2\pi i}\right)^2 \\ &\times \int_{L_1} \Gamma\left(\frac{t}{r}+\frac{as}{2}\right) \frac{\Gamma(\xi^2+t)\Gamma(\alpha+t)\Gamma(\beta+t)\Gamma(1-\frac{t}{r})\Gamma(A+\frac{t}{r})}{\Gamma(\xi^2+1+t)\Gamma(1+\frac{t}{r})} \left(\frac{(\mu_r)^{\frac{1}{r}}}{\alpha\beta}\right)^{t} dt \\ &\times \int_{L_2} \frac{\Gamma(m_s+s)\Gamma(\mu-s)\Gamma(-s)\Gamma(1-\frac{as}{2})}{\Gamma(1-s)\Gamma(1+A)} \left(\frac{\mu(\lambda C_R)^{\frac{a}{2}}}{(m_s-1)\overline{\gamma}^{\frac{a}{2}}}\right)^{s} ds\Big) \end{aligned} \tag{39}$$

The proof is completed with the help of [40, Eq.(1.1)]. ■

It should be mentioned that when $a=2$, $m_s=\infty$, $r=1$, the effective capacity in (38) can be reduced to [20, Eq. (40)].

2) DF Relaying

By using [38, Eq. (1.43)], $(1+\gamma)^{-A-1}$ can be represented in term of the Fox's H-function as $H_{1,1}^{1,1}\left[\gamma \middle| \begin{matrix}(-A,1)\\(0,1)\end{matrix}\right]$. Furthermore, by substituting (17) into (38) and utilizing [40, Eq. (2.3)], [46, Eq. (2.25.1/1)], we obtain the effective capacity of DF relaying for this system as (39), see the top of the next page.

Similarly, let us set $a=2$, $m_s=\infty$, $r=1$, as special case, (39) can be simplified to [20, Eq. (47)]

V. NUMERICAL RESULTS AND DISCUSSIONS

In this section, we provide some illustrative numerical examples of the closed-form expressions given in the previous

$$\overline{C}^{AF} = \frac{\xi^2}{2r\ln(2)\Gamma(\alpha)\Gamma(\beta)}\frac{1}{\Gamma(m)\Gamma(\mu)}H_{1,0:2,3:4,3}^{0,1:3,1:1,4} \times \left[\begin{array}{c|c|c|c} (1,\frac{a}{2},\frac{1}{r}) & (1-m_s,1)(1,1) & (1,\frac{1}{r})\,(1-\xi^2,1)\,(1-\alpha,1)\,(1-\beta,1) & \frac{\mu\lambda^{\frac{a}{2}}C_R^{\frac{a}{2}}}{(m_s-1)\bar{\gamma}^{\frac{a}{2}}},\frac{(\mu_r c)^{\frac{1}{r}}}{\alpha\beta} \\ - & (\mu,1)\,(0,1)\,(1,\frac{a}{2}) & (1,\frac{1}{r})\,(-\xi^2,1)\,(0,\frac{1}{r}) & \end{array}\right]. \tag{35}$$

$$\bar{C}^{DF} = \frac{c\xi^2}{2\ln(2)\Gamma(\alpha)\Gamma(\beta)}\frac{1}{\Gamma(m)\Gamma(\mu)}\frac{\mu_r}{(\alpha\beta)^r}H_{4,2:1,1:2,2}^{0,4:1,1:2,1} \times \left[\begin{array}{cc|c|c|c} (0,1,\frac{a}{2}) & (1-\xi^2-r,r,\frac{ar}{2}) & (1-\alpha-r,r,\frac{ar}{2})\,(1-\beta-r,r,\frac{ar}{2}) & (0,1) & (1-m_s,1)\,(1,1) \\ & (-\xi^2-r,r,\frac{ar}{2}) & (-1,1,\frac{a}{2}) & (0,1) & (\mu,1)\,(0,1) \end{array}\right|\left.\begin{array}{c} \frac{\mu_r c}{(\alpha\beta)^r},\frac{\lambda^{\frac{a}{2}}\mu_r^{\frac{a}{2}}}{(m_s-1)\bar{\gamma}^{\frac{a}{2}}(\alpha\beta)^{\frac{ar}{2}}} \end{array}\right]. \tag{37}$$

section, which study the influence of the key system parameters on the mixed FSO/RF system performance. Analytical results are verified for its correctness by means of Monte Carlo simulations. Although the same average SNR values are assumed for different hop counts in these figures, this supposition is not an essential constraint for the derivation given. For the FSO link, we take the following parameters into consideration respectively for strong and moderate atmospheric turbulence under various effects of pointing errors [20]:

$$\alpha = 3.446, \beta = 1.032, \xi = 0.893;$$
$$\alpha = 5.42, \beta = 3.8, \xi = 5.0263.$$

Fig. 2 is plotted for the effects of the turbulence-induced fading as well as the pointing errors on the end-to-end outage probability of the FSO/RF system. The RF link is subject to α-$\mathcal{F}$ fading distribution ($a = 1.85, \mu = 2.5, m_s = 5$), while various pointing error and turbulence parameters are considered by FSO link. Moreover, the relay gain factor CR is fixed to 1.7 and γ_{th} = 10 dB. We can see that under AF relay, the outage probability deteriorates by decreasing the turbulence fading parameter, (i.e., smaller α and β), or reducing the pointing error parameter, (i.e., for smaller ξ). The results also show that the asymptotic expansion in (12) follows the slope of the outage curves at high SNR. One can ascertain that the numerical results and the Monte-Carlo simulations match tightly over the entire range of average SNR showing the accuracy of (11).

The outage performance under moderate turbulence conditions and negligible pointing error is depicted in Fig. 3. The predefined threshold value is set as γ_{th} = 10 dB. We can find that under DF relay, the outage performance degrades as m_s declines, which represents the shadowing condition becomes more severe. The increase of multipath clusters (μ) also helps surmount the impacts of fading. Furthermore, the impact of μ on the outage probability is more pronounced than that of m_s. Fig. 3 also reveals that the asymptotic results in (19), (20), and (21) follow the slope of the outage curves at high SNR values. Besides, the Monte-Carlo simulations are in outstanding identity with the numerical results, which give proof of the analysis.

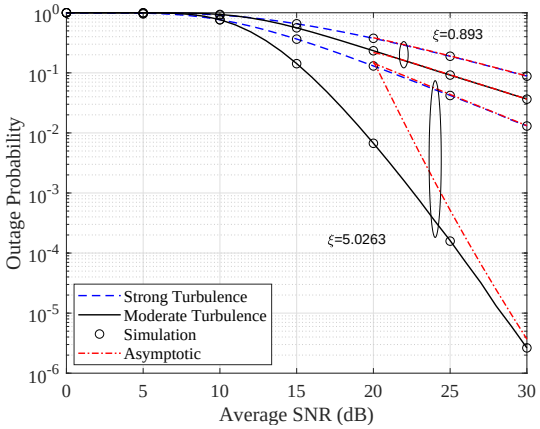

FIGURE 2. Outage probability versus average SNR each hop for strong or negligible pointing errors of a dual-hop mixed FSO/RF system using AF relaying under different turbulence conditions with heterodyne detection ($a = 1.85, \mu = 2.5$, and $m_s = 5$).

Fig. 4 presents the BER for the mixed FSO/RF system under uniform turbulence conditions and pointing error. We can see from this picture that the analysis result of the average BER closely matches the Monte Carlo simulation result, and it also shows the asymptotic result of the high SNR value in (32). Expectedly, it can be inferred from Fig.3 that for the same value of a (i.e. the non-linearity parameter of the propagation media), as the number of multipath clusters (μ) increases, the BER ameliorate and vice versa. Besides, it can also be observed that parameter a has a certain impact on the performance of the considered system.

Fig. 5 illustrates the exact formula for the BER in (31), together with the asymptotic approximation in (32) against the average SNR for a mixed FSO/RF system assuming DBPSK modulation. It can be seen that under DF relay, heterodyne detection outperforms IM/DD detection technology. Also, the impacts of atmospheric turbulence conditions can be observed in Fig. 5, as the effect of turbulence conditions gets severe, the BER deteriorates and vice versa.

In Fig. 6, the ergodic capacity under different shadowing conditions for strong and negligible pointing error with heterodyne ($r = 1$) detection techniques is presented. According

$$R^{AF} = -\frac{1}{A}\log_2\left(1 - \frac{\xi^2}{r\Gamma(\alpha)\Gamma(\beta)\Gamma(A)\Gamma(\mu)\Gamma(m_s)}H_{1,0:2,3:4,3}^{0,1:3,1:1,4} \times \left[\begin{array}{c|c|c|c} (1,\frac{a}{2},\frac{1}{r}) & (1-m_s,1)(1,1) & (1-A,\frac{1}{r})\,(1-\xi^2,1)\,(1-\alpha,1)\,(1-\beta,1) & \frac{\mu\lambda^{\frac{a}{2}}C_R^{\frac{a}{2}}}{(m_s-1)\bar{\gamma}^{\frac{a}{2}}},\frac{(\mu_r)^{\frac{1}{r}}}{\alpha\beta} \\ - & (\mu,1)\,(0,1)\,(1,\frac{a}{2}) & (1,\frac{1}{r})\,(-\xi^2,1)\,(0,\frac{1}{r}) & \end{array}\right]\right). \tag{38}$$

$$R^{DF} = -\frac{1}{A}\log_2\left(1 - \frac{\xi^2}{\Gamma(\alpha)\Gamma(\beta)}\frac{1}{\Gamma(m)\Gamma(\mu)\Gamma(A)}\frac{\mu_r}{(\alpha\beta)^r}H_{4,2:1,1:2,2}^{0,4:1,1:2,1} \times \left[\begin{matrix}(0,1,\frac{a}{2})\,(1-\xi^2-r,r,\frac{ar}{2})\,(1-\alpha-r,r,\frac{ar}{2})\,(1-\beta-r,r,\frac{ar}{2}) \\ (-\xi^2-r,r,\frac{ar}{2})\,(-1,1,\frac{a}{2})\end{matrix}\middle|\begin{matrix}(-A,1) \\ (0,1)\end{matrix}\middle|\begin{matrix}(1-m_s,1)\,(1,1) \\ (\mu,1)\,(0,1)\end{matrix}\middle|\frac{\mu_r}{(\alpha\beta)^r}, \frac{\mu\lambda^{\frac{a}{2}}\mu_r^{\frac{a}{2}}}{(m_s-1)\bar{\gamma}^{\frac{a}{2}}(\alpha\beta)^{\frac{ar}{2}}}\right]\right). \tag{39}$$

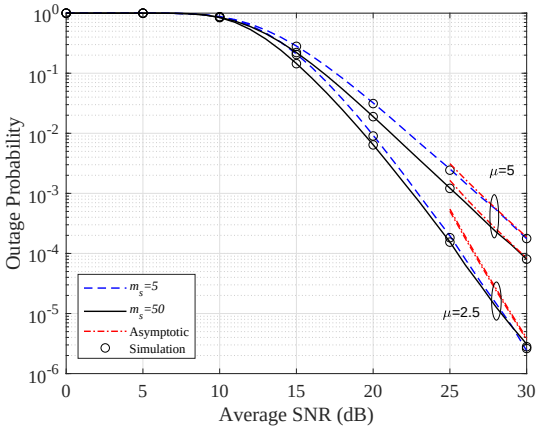

FIGURE 3. Outage probability versus average SNR each hop for different values of μ of a dual-hop mixed FSO/RF system using DF relaying under different shadowing conditions (m_s) with heterodyne detection ($a = 1.85, \xi = 5.0263, \alpha = 5.42, \beta = 3.8$).

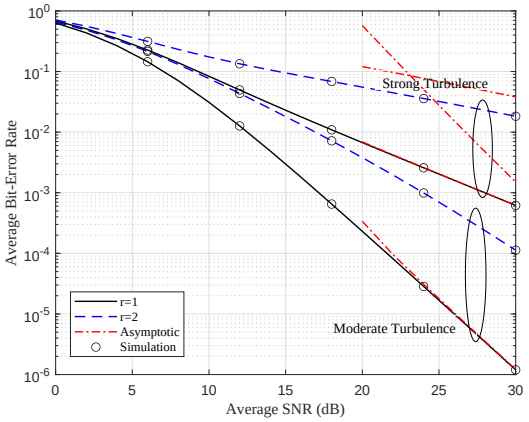

FIGURE 5. Average BER of DBPSK modulation comparing the performance of a dual-hop mixed FSO/RF system using DF relaying for different turbulence conditions under IM/DD ($r = 2$) and heterodyne ($r = 1$) techniques ($\xi = 5.0263, a = 1.85, m_s = 5, \mu = 2.5$).

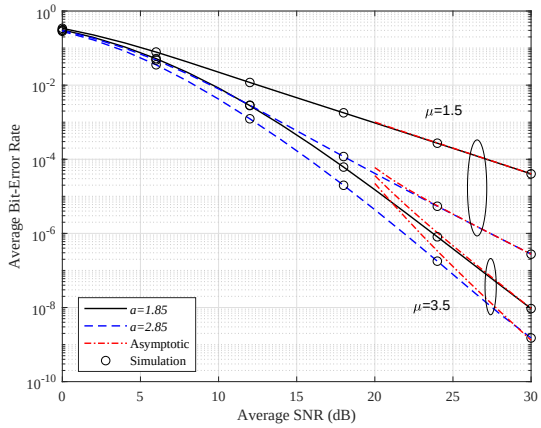

FIGURE 4. Average BER of CBPSK modulation comparing the performance of the considered DF relay system, under heterodyne techniques. Showing the impact for different values of non-linearity parameter (a) and the number of multipath clusters (μ) in the RF link ($\xi = 5.0263, m_s = 5, \alpha = 5.42, \beta = 3.8$).

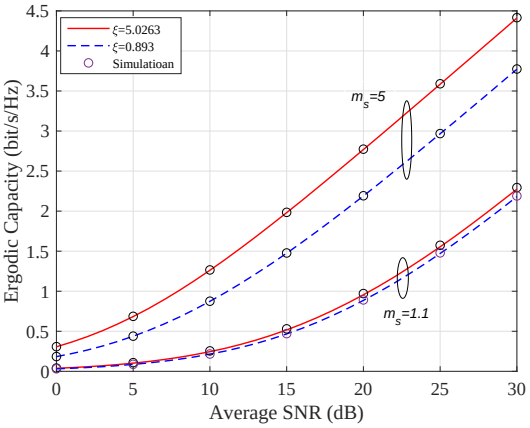

FIGURE 6. Ergodic capacity for strong and negligible pointing errors of an asymmetric FSO/RF dual-hop relaying systems using DF relaying under heterodyne techniques. Showing the impact for different values of the shadowing parameter (m_s) in the RF link ($\alpha = 5.42, \beta = 3.8, \mu = 2.5, a = 1.85$).

to the figure, we can observe that the numerical consequences are in favourable consensus with the Monte-Carlo simulations. It can be shown that similar to ξ, the ergodic capacity gain degrades as the shadowing parameter (m_s) decreases. In addition, for the heavy ($m_s = 1.1$) shadowing conditions, the ergodic capacity curves are less sensitive with respect to the value of ξ, which means that increasing ξ has less impact on the dual-hop FSO/RF system performance. This is because the scheme depends more on the RF link for communication when the pointing error is moderate or strong. We can also see that the FSO path will operate most of the time when RF linkąs quality is superior.

Fig. 7 compares the effective capacity gain against varying values of A when different turbulence conditions and various values of the parameter μ are considered. From (39), one can see that A is inversely proportional to R, which is also verified in the figure. Similarly, in Fig. 6, as the turbulence conditions become moderate, the effective capacity starts to ameliorate. Also, the impact of the number of multipath clusters can be observed. Note that as the value of μ increases (i.e. the number of multipath clusters increases) the ergodic

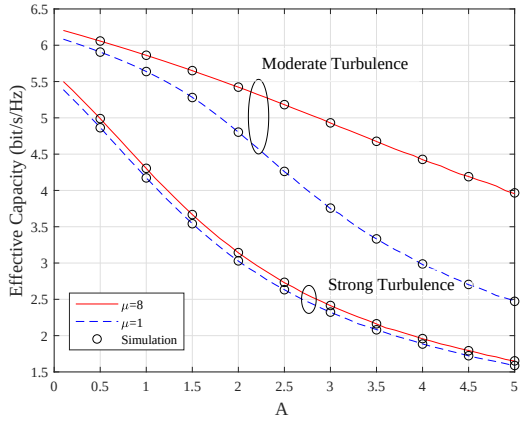

FIGURE 7. Effective capacity of an asymmetric FSO/RF dual-hop relaying systems using DF relaying under different turbulence conditions with heterodyne detection. Showing the impact for different values of μ in the RF link ($\xi = 5.0263, a = 1.85, m_s = 5$).

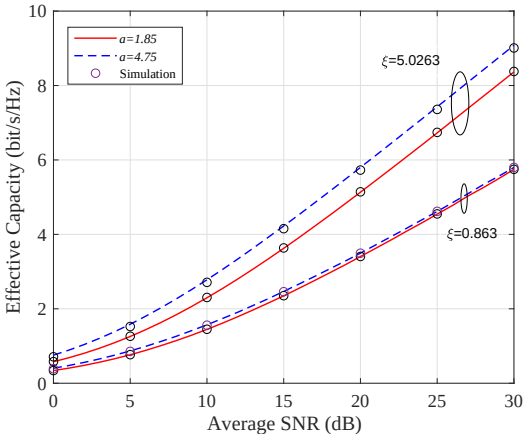

FIGURE 8. Effective capacity for strong and negligible pointing errors of an asymmetric FSO/RF dual-hop relaying systems using DF relaying with heterodyne detection. Showing the impact for different values of a in the RF link ($\alpha = 5.42, \beta = 3.8, \mu = 2.5, m_s = 5, A = 1$).

capacity improves as a result of the increased channel diversity.

In Fig. 8, perfect consistency can be noticed between the derived results (39) and Monte-Carlo simulations, which proves the accuracy of the obtained expressions. As anticipated, the effective capacity monotonically increases as average SNR, ξ, and a increase. Besides, the gap between the curves is narrower when values a increase at strong pointing errors. This implies that the bigger ξ is, the more pronounced the multipath clusters' effect will be.

VI. CONCLUSION

In this paper, the performance of dual-hop FSO/RF communication scheme considers both IM/DD and heterodyne detection has been investigated. The FSO link suffers from Gamma-Gamma fading including the effects of atmospheric turbulence with pointing errors, while RF links follow α-$\mathcal{F}$ distribution. We then derived novel accurate closed-form expressions for the OP, average BEP, effective capacity, and ergodic capacity of the end-to-end link in terms of the bivariate Fox's H-function for both AF and DF relays. In addition, we have given very compact asymptotic results in terms of common elementary functions for the acquired performance metrics at a high SNR regime and obtained diversity orders. As shown in the asymptotic results the diversity orders for the end-to-end transmission are related to the non-linearity parameter of the propagation media, the number of multipath clusters, pointing error, detection method, and turbulence parameters. We also verified the effect of fading figures of both FSO and RF links on the system performance. Expectedly, strong atmospheric turbulence and severe pointing errors can deteriorate the system performance, while heterodyne techniques, AF relaying, more multipath clusters, as well as an increase of both non-linearity and shadowing parameters, can ameliorate the system performance.

.

APPENDIX A PROOF OF COROLLARY 1

In this appendix, based on (1), we present the CDF of the end-to-end SNR γ^{AF} as

$$\begin{aligned} F_{\gamma^{AF}}(\gamma) &= \int_0^\infty P_r\left[\frac{\gamma_1\gamma_{\text{RF}}}{\gamma_{\text{RF}}+C_R} < \gamma \,|\gamma_1\right] f_{\gamma_{\text{FSO}}}(\gamma_1)d\gamma_1 \\ &= F_{\gamma_{\text{FSO}}}(\gamma) + \int_\gamma^\infty F_{\gamma_{\text{RF}}}\left(\frac{C_R\gamma}{t-\gamma}\right) f_{\gamma_{\text{FSO}}}(t)dt, \end{aligned} \tag{A.1}$$

Using the variable substitution $\gamma_1 = t - \gamma$, (A.1) can be rewritten as

$$F_{\gamma^{AF}}(\gamma) = 1 - \int_0^\infty f_{\gamma_{\text{FSO}}}(\gamma_1+\gamma)\left[1 - F_{\gamma_{\text{RF}}}\left(\frac{C_R\gamma}{\gamma_1}\right)\right]d\gamma_1, \tag{A.2}$$

Substituting (3) and (10) in (A.2), and using the primary definition of the Meijer's G-function in [36, Eq.(9.301)], we obtain

$$\begin{aligned} F_{\gamma^{AF}}(\gamma) &= 1 - \frac{\xi^2}{r\Gamma(\alpha)\Gamma(\beta)\Gamma(\mu)\Gamma(m_s)}\int_0^\infty (\gamma_1+\gamma)^{\frac{s_2}{r}-1}\gamma_1^{\frac{as}{2}}d\gamma_1 \\ &\times \left(\frac{1}{2\pi i}\right)^2 \int_{L_1} \frac{\Gamma(\xi^2-s_2)\Gamma(\alpha-s_2)\Gamma(\beta-s_2)}{\Gamma(\xi^2+1-s_2)}\left(\frac{\alpha\beta}{\mu_r^{\frac{1}{r}}}\right)^{s_2} ds_2 \\ &\times \int_{L_2} \frac{\Gamma(m_s-s_1)\Gamma(\mu+s_1)\Gamma(s_1)}{\Gamma(1+s_1)}\left(\frac{(m_s-1)\bar{\gamma}^{\frac{a}{2}}}{\mu(\lambda C_R)^{\frac{a}{2}}}\right)^{s_1} ds_1, \end{aligned} \tag{A.3}$$

where the contour L_1 and L_2 are in the s-plane and the t-plane running from $-i\infty$ to $+i\infty$, respectively. Using the [36, Eq.(3.194/3) , [Eq.(8.384/1)], $\int_0^\infty (\gamma_1+\gamma)^{\frac{s_2}{r}-1}\gamma_1^{\frac{as}{2}}d\gamma_1$ reduces to $\frac{\Gamma(1+\frac{as}{2})\Gamma(-\frac{s_2}{r}-\frac{as}{2})}{\Gamma(1-\frac{s_2}{r})}\gamma^{\frac{as}{2}+\frac{s_2}{r}}$. Then by the change of integral variable $t = -s_2$ and $s = -s_1$, (A.3) rewrites as

$$\begin{aligned} F_{\gamma^{AF}}(\gamma) &= 1 - \frac{\xi^2}{r\Gamma(\alpha)\Gamma(\beta)\Gamma(\mu)\Gamma(m_s)}\left(\frac{1}{2\pi i}\right)^2 \\ &\times \int_{L_1} \Gamma\left(\frac{t}{r}+\frac{as}{2}\right)\frac{\Gamma(\xi^2+t)\Gamma(\alpha+t)\Gamma(\beta+t)}{\Gamma(\xi^2+1+t)\Gamma(1+\frac{t}{r})}\left(\frac{(\mu_r)^{\frac{1}{r}}}{\alpha\beta}\right)^t dt \\ &\times \int_{L_2} \frac{\Gamma(m_s+s)\Gamma(\mu-s)\Gamma(-s)\Gamma(1-\frac{as}{2})}{\Gamma(1-s)}\left(\frac{\mu(\lambda C_R)^{\frac{a}{2}}}{(m_s-1)\bar{\gamma}^{\frac{a}{2}}}\right)^s ds. \end{aligned} \tag{A.4}$$

Finally, using [40, Eq. (1.1)], the CDF in (11) is obtained. Hence, the proof is completed.

APPENDIX B HIGH SNR ANALYSIS

Base on (A.4), using the definition of the H-Function [37, Eq. (1.1.2)], the CDF can be derived as

$$F_{\gamma_{AF}}(\gamma) \approx 1 - \frac{\xi^2}{2r\Gamma(\alpha)\Gamma(\beta)\Gamma(\mu)\Gamma(ms)} \frac{1}{2\pi i} \int_{L_1} \frac{\Gamma(\xi^2+t)\Gamma(\alpha+t)\Gamma(\beta+t)}{\Gamma(\xi^2+1+t)\Gamma(1+\frac{t}{r})} \times \left(\frac{\left(\frac{\mu_r}{\gamma}\right)^{\frac{1}{r}}}{\alpha\beta} \right)^t H_{3,3}^{2,3}\left(\frac{(m_s-1)\overline{\gamma}^{\frac{a}{2}}}{\mu(\lambda C_R)^{\frac{a}{2}}} \middle| \begin{matrix} (1-\mu,1)\,(1,1)\,\left(0,\frac{a}{2}\right) \\ (m_s,1)\,\left(\frac{t}{r},\frac{a}{2}\right)\,(0,1) \end{matrix} \right) dt - \frac{\xi^2}{2r\Gamma(\alpha)\Gamma(\beta)\Gamma(\mu)\Gamma(m_s)} \frac{1}{2\pi i} \int_{L_2} \frac{\Gamma(m_s+s)\Gamma(\mu-s)\Gamma(-s)\Gamma(1-\frac{as}{2})}{\Gamma(1-s)} \times \left(\frac{\mu(\lambda C_R)^{\frac{a}{2}}}{(m_s-1)\overline{\gamma}^{\frac{a}{2}}} \right)^s H_{2,4}^{4,0}\left(\alpha\beta\left(\frac{\gamma}{\mu_r}\right)^{\frac{1}{r}} \middle| \begin{matrix} \left(\xi^2+1,1\right)\,\left(1,\frac{1}{r}\right) \\ \left(\frac{as}{2},\frac{1}{r}\right)\,\left(\xi^2,1\right)\,(\alpha,1)\,(\beta,1) \end{matrix} \right) ds. \tag{B.1}$$

Additionally, for high values of μ_r and $\overline{\gamma}$, by using [37, Eq.(1.5.10) , Eq.(1.8.5)] Fox's H-functions in (B.1) can be approximated as

$$\begin{aligned} & H_{2,4}^{4,0}\left(\alpha\beta\left(\frac{\gamma}{\mu_r}\right)^{\frac{1}{r}} \middle| \begin{matrix} \left(\xi^2+1,1\right),\left(1,\frac{1}{r}\right) \\ \left(\frac{as}{2},\frac{1}{r}\right),\left(\xi^2,1\right),(\alpha,1),(\beta,1) \end{matrix} \right) \\ & \approx \frac{r\Gamma(\xi^2-\frac{asr}{2})\Gamma(\alpha-\frac{asr}{2})\Gamma(\beta-\frac{asr}{2})}{\Gamma(1+\xi^2-\frac{asr}{2})\Gamma(1-\frac{as}{2})} \left(\alpha\beta\left(\frac{\gamma}{\mu_r}\right)^{\frac{1}{r}} \right)^{\frac{asr}{2}} \\ & + \frac{\Gamma(\frac{as}{2}-\frac{\xi^2}{r})\Gamma(\alpha-\xi^2)\Gamma(\beta-\xi^2)}{\Gamma(1-\frac{\xi^2}{r})} \left(\alpha\beta\left(\frac{\gamma}{\mu_r}\right)^{\frac{1}{r}} \right)^{\xi^2} \\ & + \frac{\Gamma(\frac{as}{2}-\frac{\alpha}{r})\Gamma(\xi^2-\alpha)\Gamma(\beta-\alpha)}{\Gamma(1+\xi^2-\alpha)\Gamma(1-\frac{\alpha}{r})} \left(\alpha\beta\left(\frac{\gamma}{\mu_r}\right)^{\frac{1}{r}} \right)^{\alpha} \\ & + \frac{\Gamma(\frac{as}{2}-\frac{\beta}{r})\Gamma(\xi^2-\beta)\Gamma(\alpha-\beta)}{\Gamma(1+\xi^2-\beta)\Gamma(1-\frac{\beta}{r})} \left(\alpha\beta\left(\frac{\gamma}{\mu_r}\right)^{\frac{1}{r}} \right)^{\beta}, \end{aligned} \tag{B.2}$$

and

$$\begin{aligned} & H_{3,3}^{2,3}\left(\frac{(m_s-1)\overline{\gamma}^{\frac{a}{2}}}{\mu(\lambda C_R)^{\frac{a}{2}}} \middle| \begin{matrix} (1-\mu,1),(1,1),\left(0,\frac{a}{2}\right) \\ (m_s,1),\left(\frac{t}{r},\frac{a}{2}\right),(0,1) \end{matrix} \right) \\ & \approx -\frac{\Gamma(m_s+\mu)\Gamma\left(1-\frac{a\mu}{2}\right)\Gamma\left(\frac{t}{r}-\frac{a\mu}{2}\right)}{\mu} \left(\frac{\mu(\lambda C_R)^{\frac{a}{2}}}{(m_s-1)\overline{\gamma}^{\frac{a}{2}}} \right)^{\mu} \\ & + \Gamma(m_s)\Gamma(\mu)\Gamma\left(\frac{t}{r}\right) \\ & - \Gamma(m_s+\tfrac{2}{a})\Gamma(\mu-\tfrac{2}{a})\Gamma(\tfrac{t}{r}-1) \left(\frac{\mu(\lambda C_R)^{\frac{a}{2}}}{(m_s-1)\overline{\gamma}^{\frac{a}{2}}} \right)^{\frac{2}{a}}. \end{aligned} \tag{B.3}$$

Substituting (B.3) and (B.2) into (B.1) with some algebraic manipulations, then (12) is obtained. Hence, the proof is completed.

APPENDIX C AVERAGE BIT-ERROR RATE

Substituting (11) into (23), the average BER can be written as

$$\begin{aligned} \overline{P_e}^{AF} &= \frac{n\delta}{2} - \frac{\delta}{2\Gamma(p)} \sum_{k=1}^{n} q_k{}^{\mathrm{p}} \frac{\xi^2}{r\Gamma(\alpha)\Gamma(\beta)\Gamma(\mu)\Gamma(m_s)} \\ & \times \left(\frac{1}{2\pi i}\right)^2 \int_{L_1} \Gamma\left(\frac{t}{r}+\frac{as}{2}\right) \frac{\Gamma(\xi^2+t)\Gamma(\alpha+t)\Gamma(\beta+t)}{\Gamma(\xi^2+1+t)\Gamma(1+\frac{t}{r})} \left(\frac{(\mu_r)^{\frac{1}{r}}}{\alpha\beta} \right)^t dt \\ & \times \int_{L_2} \frac{\Gamma(m_s+s)\Gamma(\mu-s)\Gamma(-s)\Gamma(1-\frac{as}{2})}{\Gamma(1-s)} \left(\frac{\mu(\lambda C_R)^{\frac{a}{2}}}{(m_s-1)\overline{\gamma}^{\frac{a}{2}}} \right)^s ds \\ & \times \int_0^{\infty} \gamma^{p-1}\gamma^{-\frac{t}{r}} \exp(-q_k\gamma) d\gamma. \end{aligned} \tag{C.1}$$

Using [36, Eq. (3.381/4)] we obtain

$$\begin{aligned} \overline{P_e}^{AF} &= \frac{n\delta}{2} - \frac{\delta}{2\Gamma(p)} \sum_{k=1}^{n} \frac{\xi^2}{r\Gamma(\alpha)\Gamma(\beta)\Gamma(\mu)\Gamma(m_s)} \\ & \times \left(\frac{1}{2\pi i}\right)^2 \int_{L_1} \Gamma\left(\frac{t}{r}+\frac{as}{2}\right) \frac{\Gamma(\xi^2+t)\Gamma(\alpha+t)\Gamma(\beta+t)\Gamma(p-\frac{t}{r})}{\Gamma(\xi^2+1+t)\Gamma(1+\frac{t}{r})} \left(\frac{(q_k\mu_r)^{\frac{1}{r}}}{\alpha\beta} \right)^t dt \\ & \times \int_{L_2} \frac{\Gamma(m_s+s)\Gamma(\mu-s)\Gamma(-s)\Gamma(1-\frac{as}{2})}{\Gamma(1-s)} \left(\frac{\mu(\lambda C_R)^{\frac{a}{2}}}{(m_s-1)\overline{\gamma}^{\frac{a}{2}}} \right)^s ds. \end{aligned} \tag{C.2}$$

The proof is completed with the help of [40, Eq. (1.1)].

REFERENCES

[1] S. Arnon, J. Barry, G. Karagiannidis, R. Schober, and M. Uysal, *Advanced optical wireless communication systems*. Cambridge Uni. press., 2012.

[2] M. Safari and M. Uysal, "Relay-assisted free-space optical communication," *IEEE Trans. Wireless Commun.*, vol. 7, no. 12, pp. 5441–5449, Dec. 2008.

[3] J. Zhang, L. Dai, Y. Han, Y. Zhang, and Z. Wang, "On the ergodic capacity of mimo free-space optical systems over turbulence channels," *IEEE J. Select. Areas Commun*, vol. 33, no. 9, pp. 1925–1934, Jul. 2015.

[4] L. C. Andrews, R. L. Phillips, and C. Y. Hopen, *Laser beam scintillation with applications*. SPIE Press, 2001, vol. 99.

[5] A. A. Farid and S. Hranilovic, "Outage capacity optimization for free-space optical links with pointing errors," *Journal of Lightwave Technology*, vol. 25, no. 7, pp. 1702–1710, Jul. 2007.

[6] I. S. Ansari, F. Yilmaz, and M.-S. Alouini, "Performance Analysis of Free-Space Optical Links Over Málaga ($\mathcal{M}$) Turbulence Channels With Pointing Errors," *IEEE Trans. Wireless Commun.*, vol. 15, no. 1, pp. 91–102, Jan. 2016.

[7] S. L. Cotton, "Human body shadowing in cellular device-to-device communications: Channel modeling using the shadowed κ-μ fading model," *IEEE J. Sel. Areas Commun.*, vol. 33, no. 1, pp. 111–119, Jan. 2015.

[8] N. Saxena, F. H. Kumbhar, and A. Roy, "Exploiting social relationships for trustworthy D2D relay in 5G cellular networks," *IEEE Commun. Mag.*, vol. 58, no. 2, pp. 48–53, Feb. 2020.

[9] R. I. Ansari, C. Chrysostomou, S. A. Hassan, M. Guizani, S. Mumtaz, J. Rodriguez, and J. J. Rodrigues, "5G D2D networks: Techniques, challenges, and future prospects," *IEEE Syst. J.*, vol. 12, no. 4, pp. 3970–3984, Dec. 2018.

[10] J. Zhang, E. Björnson, M. Matthaiou, D. W. K. Ng, H. Yang, and D. J. Love, "Prospective multiple antenna technologies for beyond 5g," *IEEE J. Select. Areas Commun*, vol. 38, no. 8, pp. 1637–1660, Jun. 2020.

[11] M. O. Hasna and M.-S. Alouini, "A performance study of dual-hop transmissions with fixed gain relays," *IEEE Trans. Wireless Commun.*, vol. 3, no. 6, pp. 1963–1968, Nov. 2004.

[12] E. Lee, J. Park, D. Han, and G. Yoon, "Performance analysis of the asymmetric dual-hop relay transmission with mixed RF/FSO links," *IEEE Photon. Technol. Lett.*, vol. 23, no. 21, pp. 1642–1644, Nov. 2011.

[13] E. Soleimani-Nasab and M. Uysal, "Generalized performance analysis of mixed RF/FSO cooperative systems," *IEEE Trans. Wireless Commun.*, vol. 15, no. 1, pp. 714–727, Jan. 2016.

[14] J. Zhang, L. Dai, Y. Zhang, and Z. Wang, "Unified performance analysis of mixed radio frequency/free-space optical dual-hop transmission systems," *J. Lightw. Technol.*, vol. 33, no. 11, pp. 2286–2293, Mar. 2015.

[15] E. Zedini, H. Soury, and M.-S. Alouini, "On the performance of dual-hop FSO/RF systems," in *Proc. IEEE Int. Symp. Wireless Commun. Syst. (ISWCS)*. IEEE, Aug. 2015, pp. 31–35.

[16] E. Zedini, I. S. Ansari, and M.-S. Alouini, "Performance analysis of mixed Nakagami-m and Gamma–Gamma dual-hop FSO transmission systems," *IEEE Photon. J.*, vol. 7, no. 1, pp. 1–20, Feb. 2015.

[17] S. Anees and M. R. Bhatnagar, "Performance evaluation of decode-and-forward dual-hop asymmetric radio frequency-free space optical communication system," *IET Optoelectron*, vol. 9, no. 5, pp. 232–240, Oct. 2015.

[18] E. Zedini, H. Soury, and M.-S. Alouini, "On the performance analysis of dual-hop mixed FSO/RF systems," *IEEE Trans. Wireless Commun.*, vol. 15, no. 5, pp. 3679–3689, May. 2016.

[19] R. Singh, M. Rawat, and A. Jaiswal, "Mixed FSO/RF SIMO SWIPT Decode-and-Forward Relaying Systems," in *2020 International Conference on Signal Processing and Communications (SPCOM)*. IEEE, Jul. 2020, pp. 1–5.

[20] Y. Zhang, J. Zhang, L. Yang, B. Ai, and M.-S. Alouini, "On the Performance of Dual-Hop Systems over Mixed FSO/mmWave Fading Channels," *IEEE Open J. Commun. Soc.*, vol. 1, pp. 477–489, May. 2020.

[21] H. Du, J. Zhang, J. Cheng, and B. Ai, "Sum of Fisher-Snedecor $\mathcal{F}$ random variables and its applications," *IEEE Open J. Commun. Soc.*, vol. 1, pp. 342–356, Mar. 2020.

[22] P. Zhang, J. Zhang, K. P. Peppas, D. W. K. Ng, and B. Ai, "Dual-hop relaying communications over Fisher-Snedecor $\mathcal{F}$-fading channels," *IEEE Trans. Commun.*, vol. 68, no. 5, pp. 2695–2710, Feb. 2020.

[23] S. Chen, J. Zhang, G. K. Karagiannidis, and B. Ai, "Effective Rate of MISO Systems Over Fisher–Snedecor mathcal $\mathcal{F}$ fading channels," *IEEE Commun. Lett*, vol. 22, no. 12, pp. 2619–2622, Dec. 2018.

[24] J. Zhang, M. Matthaiou, G. K. Karagiannidis, and L. Dai, "On the multivariate gamma–gamma distribution with arbitrary correlation and applications in wireless communications," *IEEE Trans. Veh. Technol.*, vol. 65, no. 5, pp. 3834–3840.

[25] E. Soleimani-Nasab and M. Uysal, "Generalized performance analysis of mixed RF/FSO systems," in *Proc. IEEE Opt. Wireless Commun. (IWOW)*. IEEE, Sept. 2014, pp. 16–20.

[26] D. R. Pattanayak, S. Rai, V. K. Dwivedi, and G. Singh, "A statistical channel model for a decode-and-forward based dual hop mixed RF/FSO relay network," *Opt Quant Electron*, vol. 50, no. 6, p. 229, May. 2018.

[27] B. Ashrafzadeh, E. Soleimani-Nasab, M. Kamandar, and M. Uysal, "A framework on the performance analysis of dual-hop mixed FSO-RF cooperative systems," *IEEE Trans. Wireless Commun.*, vol. 67, no. 7, pp. 4939–4954, Jul. 2019.

[28] H. Samimi and M. Uysal, "End-to-end performance of mixed RF/FSO transmission systems," *IEEE/OSA J. Opt. Commun. Netw*, vol. 5, no. 11, pp. 1139–1144, Nov. 2013.

[29] P. V. Trinh, T. C. Thang, and A. T. Pham, "Mixed mmwave RF/FSO relaying systems over generalized fading channels with pointing errors," *IEEE/OSA Photon. J.*, vol. 9, no. 1, pp. 1–14, Feb. 2016.

[30] U. Anushree and V. Jagadeesh, "Outage Performance Analysis of Hybrid FSO/RF System Using Rayleigh and K-Distribution," in *Advances in Communication, Signal Processing, VLSI, and Embedded Systems*. Springer, 2020, pp. 69–78.

[31] I. Trigui, N. Cherif, S. Affes, X. Wang, V. Leung, and A. Stephenne, "Interference-limited mixed Málaga-$\mathcal{M}$ and generalized-$\mathcal{K}$ dual-hop FSO/RF systems," in *Proc. IEEE Annu. Int. Symp. Pers., Indoor, Mobile Radio Commun., Montreal, QC, Canada*. IEEE, Oct. 2017, pp. 1–6.

[32] O. Badarneh, "The $\alpha - \mathcal{F}$ Composite Fading Distribution: Statistical Characterization and Applications," *IEEE Trans. Veh. Technol.*, May. 2020.

[33] B. Xia, Y. Fan, J. Thompson, and H. V. Poor, "Buffering in a three-node relay network," *IEEE Trans. Wirless Commun*, vol. 7, no. 11, pp. 4492–4496, Dec. 2008.

[34] N. Zlatanov, R. Schober, and P. Popovski, "Buffer-aided relaying with adaptive link selection," *IEEE J. Select. Areas Commun*, vol. 31, no. 8, pp. 1530–1542, Oct. 2012.

[35] W. Gappmair, "Further results on the capacity of free-space optical channels in turbulent atmosphere," *IET Commun*, vol. 5, no. 9, pp. 1262–1267, May. 2011.

[36] I. S. Gradshteyn and I. M. Ryzhik, *Table of integrals, series, and products*. Academic press, 2014.

[37] A. A. Kilbas, *H-transforms: Theory and Applications*. CRC Press, 2004.

[38] R. K. S. A. Mathai and H. J. Haubold, *The H-function: Theory and Applications*. New York, NY, USA: Springer, 2010.

[39] F. W. Olver, D. W. Lozier, R. F. Boisvert, and C. W. Clark, *NIST handbook of mathematical functions hardback and CD-ROM*. Cambridge university press, 2010.

[40] P. Mittal and K. Gupta, "An integral involving generalized function of two variables," in *Proceedings of the Indian academy of sciences-section A*, vol. 75, no. 3. Springer, 1972, pp. 117–123.

[41] K. P. Peppas, "A new formula for the average bit error probability of dual-hop amplify-and-forward relaying systems over generalized shadowed fading channels," *IEEE Wireless Commun. Lett.*, vol. 1, no. 2, pp. 85–88, Apr. 2012.

[42] B. Bag, A. Das, C. Bose, and A. Chandra, "Improving the performance of a DF relay-aided FSO system with an additional source–relay mmwave RF backup," *J. Opt. Commun. Netw.*, vol. 12, no. 12, pp. 390–402, Dec. 2020.

[43] E. Zedini, H. Soury, and M.-S. Alouini, "Dual-hop FSO transmission systems over Gamma–Gamma turbulence with pointing errors," *IEEE Trans. Wireless Commun.*, vol. 16, no. 2, pp. 784–796, Feb. 2017.

[44] H. Z.-J. Hamid Arezumand and E. Soleimani-Nasab, "Outage and Diversity Analysis of Underlay Cognitive Mixed RF-FSO Cooperative Systems," *J. Opt. Commun. Netw.*, vol. 9, no. 10, pp. 909–920, Oct 2017.

[45] Z. Wang and G. B. Giannakis, "A simple and general parameterization quantifying performance in fading channels," *IEEE Trans. Commun*, vol. 51, no. 8, pp. 1389–1398, Aug. 2003.

[46] A. P. Prudnikov, J. A. Bryčkov, and O. I. Maričev, *Integrals and series. Vol. 3, More special functions*. Gordon and Breach, 2003.

[47] A. Lapidoth, S. M. Moser, and M. A. Wigger, "On the capacity of free-space optical intensity channels," *IEEE Trans. Inf. Theory*, vol. 55, no. 10, pp. 4449–4461, Oct. 2009.

Qiang Sun received the Ph.D. degree in communications and information systems from Southeast University, Nanjing, in 2014. He was a Visiting Scholar with the University of Delaware, USA, in 2016. He is currently an Associate Professor with the School of Information Science and Technology, Nantong, China. His research interests include deep learning and wireless communications.

ZIHAN ZHANG is currently pursuing the M.S. degree in Information Science and Technology with Nantong University, China. Her research interests include performance analysis of wireless communication systems.

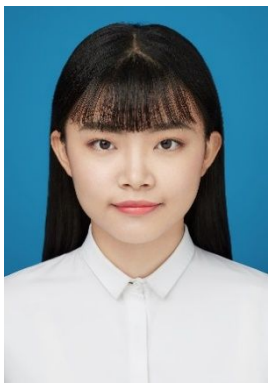

YAN ZHANG is currently pursuing the master's degree in communications engineering with Beijing Jiaotong University, Beijing, China. Her research interests include reconfigurable intelligent surface and performance analysis of wireless communication systems.

MIGUEL LÓPEZ-BENÍTEZ (Senior Member, IEEE) received the B.Sc. and M.Sc. degrees (Hons.) in telecommunication engineering from Miguel Hernández University, Elche, Spain, in 2003 and 2006, respectively, and the Ph.D. degree (summa cum laude) in telecommunication engineering from the Technical University of Catalonia, Barcelona, Spain, in 2011. From 2011 to 2013, he was a Research Fellow with the Centre for Communication Systems Research, University of Surrey, Guildford, U.K. In 2013, he became a Lecturer (Assistant Professor) with the Department of Electrical Engineering and Electronics, University of Liverpool, U.K., where he has been a Senior Lecturer (Associate Professor) since 2018. His research interests include the field of wireless communications and networking, with special emphasis on mobile communications and dynamic spectrum access in

cognitive radio systems. He has been the Principal Investigator or a Co-Investigator of research projects funded by the EPSRC, British Council, and Royal Society. He has also been involved in the European-funded projects AROMA, NEWCOM++, FARAMIR, QoSMOS, and CoRaSat. He has also been a member of the Organising Committee for the IEEE WCNC International Workshop on Smart Spectrum since 2015. He is also an Associate Editor of IEEE ACCESS, IET Communications, and Wireless Communications and Mobile Computing.

Jiayi Zhang (S'08–M'14–SM'20) received the B.Sc. and Ph.D. degree of Communication Engineering from Beijing Jiaotong University, China in 2007 and 2014, respectively. Since 2016, he has been a Professor with School of Electronic and Information Engineering, Beijing Jiaotong University, China. From 2014 to 2016, he was a Postdoctoral Research Associate with the Department of Electronic Engineering, Tsinghua University, China. From 2014 to 2015, he was also a Humboldt Research Fellow in Institute for Digital Communications, Friedrich-Alexander-University Erlangen-Nurnberg (FAU), Germany. From 2012 to ¨ 2013, he was a visiting scholar at the Wireless Group, University of Southampton, United Kingdom. His current research interests include massive MIMO, large intelligent surface, communication theory and applied mathematics. Dr. Zhang received the Best Paper Awards at the WCSP 2017 and IEEE APCC 2017. He was recognized as an exemplary reviewer of the IEEE COMMUNICATIONS LETTERS in 2015 and 2016. He was also recognized as an exemplary reviewer of the IEEE TRANSACTIONS ON COMMUNICATIONS in 2017-2019. He was the Lead Guest Editor of the special issue on "Multiple Antenna Technologies for Beyond 5G" of the IEEE JOURNAL ON SELECTED AREAS IN COMMUNICATIONS in 2020. He currently serves as an Associate Editor for IEEE TRANSACTIONS ON COMMUNICATIONS, IEEE COMMUNICATIONS LETTERS, IEEE ACCESS and IET COMMUNICATIONS.